21

Efficient THz emission by a photoconductive emitter with tight photocarrier confinement within high-aspect ratio plasmonic electrodes

© D.S. Ponomarev[1,2,3], D.V. Lavrukhin[1,2], A.E. Yachmenev[1,2], R.R. Galiev[1], R.A. Khabibullin[1,2,3], Yu.G. Goncharov[4], K.I. Zaytsev[4]

[1] Institute of Ultra High Frequency Semiconductor Electronics of RAS, Moscow, Russia
[2] Bauman Moscow State Technical University, Moscow, Russia
[3] Moscow Institute of Physics and Technology (National Research University), Dolgoprudny, Moscow Region, Russia
[4] Prokhorov General Physics Institute of the Russian Academy of Sciences, Moscow, Russia

e-mail: ponomarev_dmitr@mail.ru

Received December 11, 2023
Revised January 09, 2024
Accepted January 16, 2024

We propose, simulate and investigate how the thickness of plasmonic electrode h and the ratio between h and the period of subwavelength periodical metallic (plasmonic) grating h/p on the THz emission efficiency in a photoconductive emitter. By numerical optimization we determine the grating geometry with respect to maximal optical transmission. We showcase that simultaneous increase in h and h/p allows efficient excitation of plasmon modes in the grating, that follows with an THz power enhancement up to 10000 compared to conventional emitter without grating. The overall THz power exceeds $5\,\mu$W in the $0.1-4$ THz bandwidth, with the conversion efficiency of $\sim 0.2\%$. The developed grating design can be also used for photoconductive THz detectors in modern THz spectroscopic and imaging setups.

Keywords: terahertz science and technology, terahertz pulsed spectroscopy, terahertz element base, photoconductive antenna, plasmonic grating, optical light confinement, semiconductors.

DOI: 10.61011/EOS.2024.01.58299.1-24

Introduction

Compact and cost-effective spectrometers and terahertz (THz) visualization systems based on photoconductive ultrashort laser pulse converters are being developed extensively and widely used for solution on fundamental and applied problems in various science and technology areas [1,2]. Thanks to their small size, simplicity and reliability for electromagnetic pulse generation and detection, modern THz spectrometers widely use photoconductive emitters and detectors [3,4]. Efficiency of spectroscopic and imaging systems is defined by key characteristics of photoconductive devices such as emission spectrum profile, overall THz emission power in the specified frequency range and signal-to-noise ratio. Most recently, unique photoconductive emitters on Ge substrates have been proposed [5]. They do not have effective absorption on optical phonons compared with GaAs. This allowed the authors to achieve a record-breaking oscillating of 70 THz bandwidth, however, at a relatively low dynamic range [6]. Beginning from the first experiments on silicon photoconductivity [7], considerable progress in photoconductive THz emitters has been achieved [4], however, the efficiency of laser pumping pulse energy conversion into THz electromagnetic oscillations is still relatively low and hinders the applicability of these devices in wideband THz spectroscopy systems. Research teams have achieved considerable success using innovative approaches. In particular, they proposed various photovoltaic THz emitters running in photo-Dember (surface) oscillation mode [8,9] (without external bias), dielectric nanoantennas [10] and plasmonic electrodes of various topology [11–13] used to enhance THz emission power, quantum dot semiconductor heterostructures [14,15] and unique materials based on topological insulators [16].

In [17], we have studied the effect of plasmonic electrode height (thickness) on spectral and power characteristics of the generated THz emission in plasmonic electrodes made using planar technology. We have shown that an increase in the electrode height up to $h = 100$ nm is accompanied by an increase in electric field strength at metal/semiconductor interface. This results in a notable increase in transient current, therefore THz emission power grows up to a factor of $\sim 10^3$ compared with a traditional emitter without plasmonic electrodes.

Herein, we have improved our previous model of plasmonic grating such that its geometrical parameters (height, width and electrode gap) are optimized to achieve maximum transmittance of a laser pumping pulse and have shown that additional 10x power amplification of THz emission is possible due to combination of simultaneous

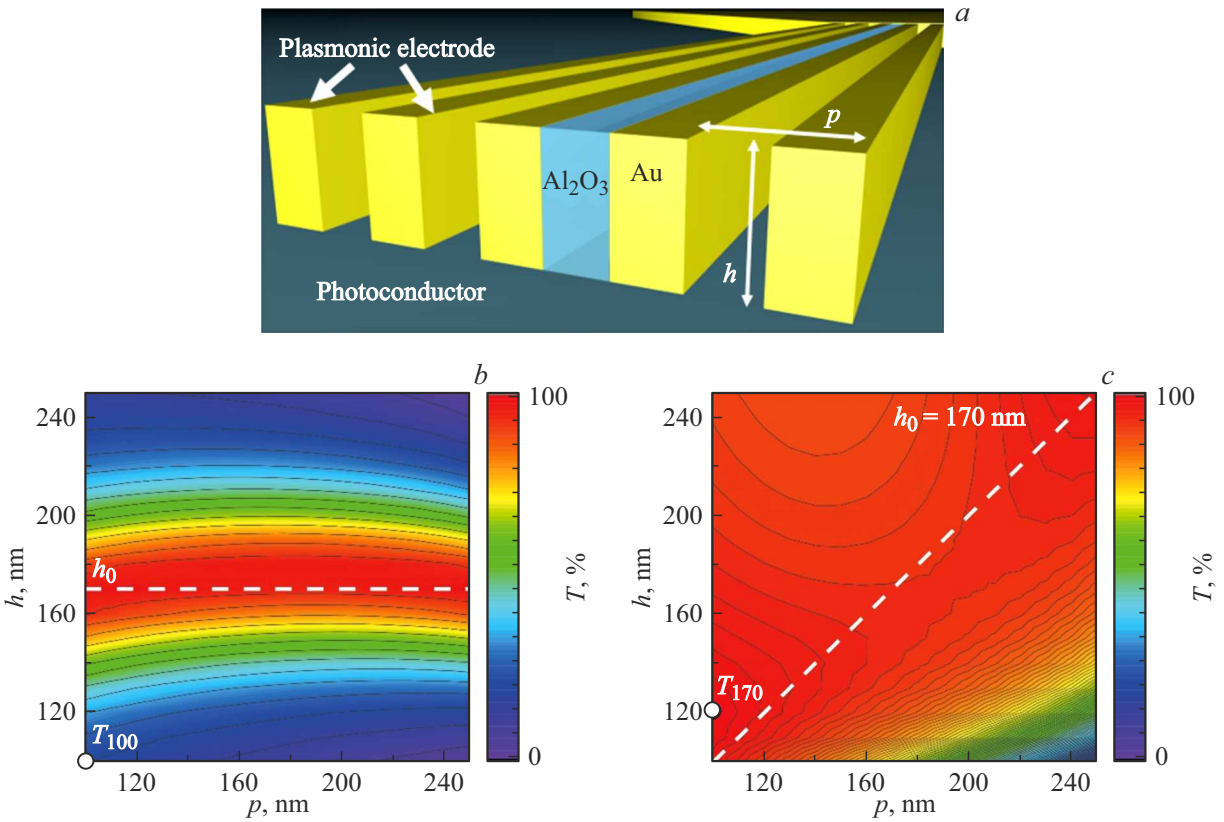

Figure 1. The proposed grating model with high aspect ratio plasmonic Au electrodes filled with a thin Al_2O_3 dielectric layer (a); calculated dependences of electrode height h on grating period p (b), as well as of the electrode gap g on electrode thickness w (c) to achieve the maximum transmittance of laser pumping emission T through the grating. $h_0 = 170$ nm corresponds to the maximum transmittance of laser pumping pulse through the grating; T_{100} and T_{170} are typical transmittance factors for the grating with electrode heights $h = 100$ nm [17] and $h = 170$ nm.

increase in the plasmonic electrode height to $h = 170$ nm and in ratio of height and grating period to $h/p \sim 0.8$. It is shown that in this case slit metal waveguides are formed in the grating where 800 nm laser pumping emission produces effective excitation of plasmon oscillations. Thanks to the selected grating topology, we have achieved a record-breaking power amplification of THz emission to a factor of 10^4 compared with a photoconductive THz emitter without grating.

Electromagnetic analysis of plasmonic grating

The electromagnetic analysis was carried out using the finite element method. The design domain represented two gold electrodes of THz emitter separated by a thin dielectric layer with periodic boundary conditions [18]. A nonuniform grid with a maximum mesh size of 5 nm and constant separation on the boundary under the grating was used. The electric field vector of a laser pumping pulse has TM polarization, i.e. it was oriented perpendicularly to the electrodes for excitation of plasma oscillations.

The grating with high aspect ratio plasmonic electrodes arranged in the THz emitter gap has an important function of polarization-selective excitation of the photoconductor. The grating geometry was optimized in order achieve the maximum transmittance of laser pumping emission — the more fraction of pumping emission flows through the grating the more charger carriers are formed in the photoconductor, thus, increasing the generated transient current pulse in the emitter and current signal in the detector. Numerical calculation was used to chose the following parameters: plasmonic electrode height (thickness) $h = 170$ nm, electrode width $w = 100$ nm, electrode gap $g = 120$ nm. Slit waveguides formed by the grating electrodes were filled with a thin layer of Al_2O_3 dielectric with an optimized thickness of 120 nm; the dielectric layer ensured reduction of Fresnel loss by reflection of laser pumping pulses from the grating to $\sim 20-30\%$ (i.e. served as antireflection optics) and provided mechanical protection of the grating due to low thickness of plasmon electrodes.

The proposed grating model and analysis results are shown in Figure 1. The model used the Drude–Lorentz dispersion model with refraction indices $n = 0.0794 + 4.835i$

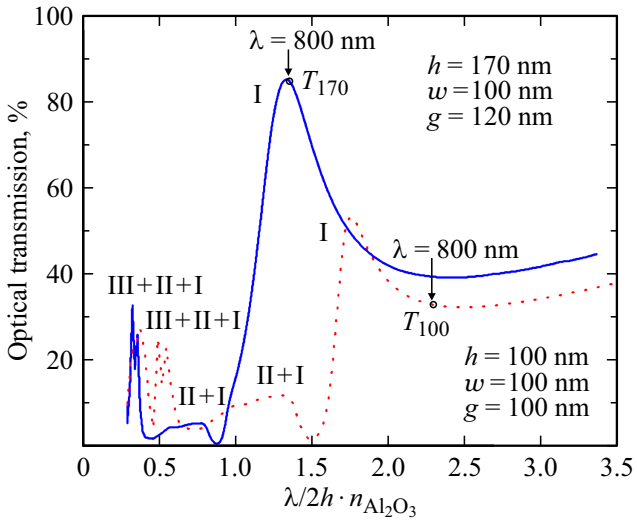

Figure 2. Change in the transmittance of the slit waveguide formed by high aspect ratio electrodes associated with excitation of plasmonic modes. Blue solid line corresponds to the proposed grating geometry with an electrode height $h = 170$ nm and aspect ratio $h/p \sim 0.8$; red dotted curve corresponds to the plasmonic grating with $h = 100$ nm and $h/p = 0.5$ [17].

and $n = 1.75$ for Au and Al_2O_3, respectively (for laser emission with a central wavelength of $\lambda = 800$ nm) [19,20]. The fact that the high aspect ratio between electrode height and grating period is equal to $h/p \sim 0.8$ is an important feature of the proposed grating. This means that slit waveguides filled with dielectric are formed in the grating [21], in our case this is Al_2O_3.

The results of numerical calculation of the transmittance factor for different slit waveguides are shown in Figure 2. $\lambda = 800$ nm laser excitation is shown by arrows near the curves. Peaks „I–III“ correspond to transmittance growth due to resonant mode excitation in the waveguide. It can be clearly seen that even the fundamental mode is not excited in the grating with $h/p \sim 0.5$ ($h = 100$ nm) on the contrary to the grating with $h/p \sim 0.8$ ($h = 170$ nm), where the arrow directly corresponds to the maximum transmittance peak that means effective excitation of the fundamental plasmonic mode. It should be noted that increase in h and h/p facilitates further THz emission power amplification , however, when the electrode thickness increases, technological difficulties occur due to lift off of the top metal (so-called *lift-off* technology [13,17]) and to „proximity effects“ when electron resist occurs. Therefore, we have chosen the best value $h/p \sim 0.8$ in terms of technology. According to the calculations, the chosen grating topology ensures transmittance up to $T_{170} = 1 - R - A \sim 0.78$ of pumping emission, while the reflectance decreases by 29% to $R \sim 0.17$ due to the use of antireflection Al_2O_3 dielectric layer, and ohmic loss in metal do not exceed $A \sim 0.05$.

Test samples and experiment

Samples of photoconductive THz emitters were made by IUHFSE RAS and had two different plasmonic gratings with electrode height $h = 100$ and 170 nm and different ratioh/p, as described in the simulation section, for comparative analysis of their spectral characteristics. A „bow tie“ topology with flare angle 60° and photoconductive gap 12 μm was used as the main electrode topology. A low-temperature grown GaAs layer was used as a photoconductor material. 500 nm plating of Au electrodes was produced by vacuum thermal evaporation method, and plasmonic electrode patterning was made using Raith Voyager system. A thin Al_2O_3 dielectric layer was applied by the atomic layer deposition method. The plasmonic grating manufacturing process is described in detail in [22,23].

The optical circuit diagram of the THz pulsed spectrometer used for characterization of the test samples is shown in Figure 3. EFOA-SH optical fiber laser (Avesta-Proekt, Russia) with central wavelength $\lambda_0 = 780$ nm, pulse width $\tau_{opt} \approx 100$ fs (FWHM), pulse repetition rate $f_{rep} = 70$ MHz and mean power ~ 100 mW was used as a femtosecond laser emitter. Laser emission was focused in the photoconductive emitter and detector gaps by similar plano-convex lens 6 mm in diameter and 10 mm in focal distance to provide a focal spot diameter up to $d \approx 4\,\mu$m. Alternating bipolar square-wave bias voltage with ajustable amplitude $U_b = 0-30$ V and frequency $f = 20$ kHz were applied to the emitter. Re-arrangement of the programmable attenuator made it possible to adjust the mean laser excitation power of the emitter or laser probing power of the detector within 0.1–30 mW. The developed THz emitters fed by square-wave pulses with amplitude $U_b = 5-12$ V were used as the source, while a commercially available TERA-8 dipole antenna (Menlo Systems) served as the detector.

Preliminary amplification of the detector current signal $I_{det}(t)$ was carried out by the current converter to voltage $U = I_{det}R_{IU}$ with equivalent resistance $R_{IU} = 10$ MΩ.

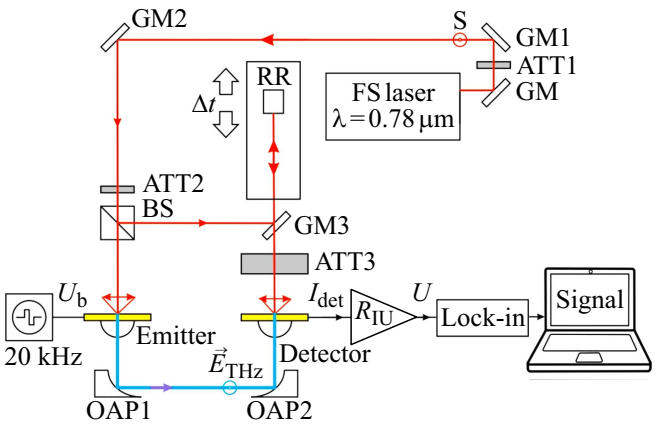

Figure 3. Optical circuit diagram for measurements of the developed photoconductive THz emitters with plasmonic gratings. GM — metal mirrors, OAP — of-axis parabolic mirrors, ATT — attenuators, BS — beam splitting cube, RR — retroreflector.

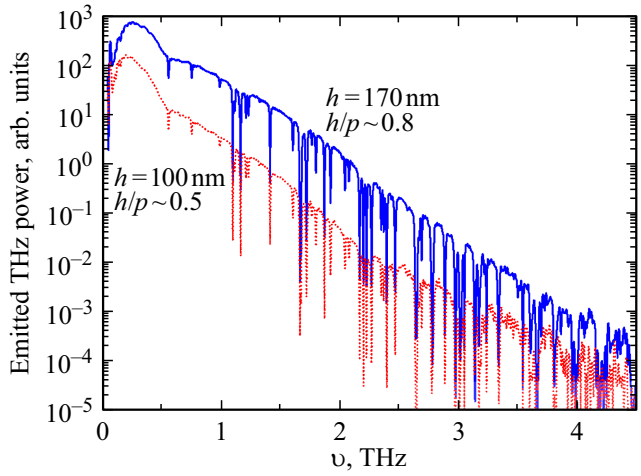

Figure 4. Spectral measurements of THz emission power for the two photoconductive emitters with different plasmonic electrode geometry: blue solid curve corresponds to the proposed grating geometry with electrode height $h = 170$ nm and aspect ratio $h/p \sim 0.8$, red dotted curve corresponds to the plasmonic grating with $h = 100$ nm and $h/p = 0.5$. The measurements were carried out at a mean power in the pumping beam $P_{opt} = 2.8$ mW and external bias on the emitter electrodes $U_b = 8$ V.

Demodulation of signal $U(t)$ at f with further 10x amplification of the RMS voltage was carried out by a synchronous amplifier with bandwidth $\Delta f = 660$ Hz and Q factor $Q = f/\Delta f \approx 30$. Electric modulation of THz emission power using the alternating bias voltage of the emitter U_b ensured high modulation frequency f that is unattainable for mechanical THz beam chopper that allowed the flicker noise in the amplifier band Δf to be reduced. Final signal conversion into digital form was performed by a 16-bit programmable analog-to-digital converter. Synchronization of all electronic units of the pulse spectrometer via a USB digital interface, measurement parameter setting, visualization of the time dependence of THz pulse electric field (THz pulse waveform) and Fourier spectrum, signal accumulation and measurement data storage were carried out using original PC software. Due to the use of delay of the translator with linear table drive motor in the optical line, high signal recording rate was achieved, i.e. THz pulse waveform measurement in time delay range $T = 67$ ps, the supporting spectral resolution $T^{-1} = 0.015$ THz in the frequency range 0.1–5.0 THz took less than 1 s (recording of one signal without averaging several instances).

Finding and discussion

Oscillation spectra of the test samples of photoconductive emitters with plasmonic gratings are shown in Figure 4. For THz measurements, the following parameters were used: mean source pumping emission power $P_{opt} = 2.8$ mW, bias voltage $U_b = 8$ V — to avoid saturation effects due to high transient current. Figure 4 shows that both curves have a similar shape, whilst the oscillating band is ~ 4 THz with signal-to-noise ratio more than 65 dB. Comparison of spectral characteristics of the samples clearly indicates almost 10x increase of the emitted THz power and corresponding increase in the signal-to-noise ratio up to +10 dB, in the emitter with plasmonic electrode height $h = 170$ nm compared with the equivalent emitter with $h = 100$ nm.

Considering the findings of our previous research [17], the total amplification in the plasmonic grating geometry developed herein is $\sim 10^4$ compared with the emitter without grating. It should be noted that increase in the transmittance factor results in the increase in the laser pumping energy absorbed by a semiconductor. In other words, more charge carriers will be generated when the semiconductor and high aspect ratio grating metal electrode contact are is exposed to laser pulse. The latter will result in amplification of the transient current and, thus, of THz emission power. Simulation results predict the transmittance ratio for two gratings $T_{170}/T_{100} \sim 0.78/0.39 = 2$ (Figure 1). Increase in THz emission power by a factor of ~ 22 shall correspond to such increase in transmittance. However, this calculation does not consider the resonant nature of electric field amplification during plasmonic mode excitation. Figure 2 shows that this is the case that occurs when the grating electrode height is $h = 170$ nm, while for the grating with $h = 100$ nm no plasmonic mode excitation takes place. Therefore, for more correct comparison of simulation with experiment, additional calculation of the transient current pulse is required by solution of charge carrier drift-diffusion equations considering the plasmonic mode excitation that is beyond the scope of the study.

Conclusion

The study offers, justifies theoretically and investigates experimentally the effect of plasmonic electrode height h and ratio of height and subwavelength periodic metal (plasmonic) grating period h/p in the photoconductive emitter on the THz emission efficiency. Numerical simulation was used to determine the optimum plasmonic grating parameters corresponding to the maximum transmittance of a laser pumping pulse through the grating. It is shown that simultaneous increase in h and h/p results in effective excitation of plasmonic modes that is followed by an increase in the THz emission power to a factor of 10^4 compared with a traditional photoconductive emitter without grating. Integral emission power is more than 5 μW in the frequency generation band 0.1–4 THz at conversion efficiency $\sim 0.2\%$.

Funding

The study was supported financially by Russian Science Foundation grant 19-79-10240.

Conflict of interest

The authors declare that they have no conflict of interest.

References

[1] D.S. Ponomarev, A.E. Yachmenev, D.V. Lavrukhin, R.A. Khabibullin, N.V. Chernomyrdin, I.E. Spektor, V.N. Kurlov, V.V. Kveder, K.I. Zaytsev. Phys. Usp., **67** (1), 3–21 (2024). DOI: 10.3367/UFNe.2023.07.039503.

[2] X. Li, J. Li, Y. Li, A. Ozcan, M. Jarrahi. Light: Sci. Appl., **12**, 233 (2023). DOI: 10.1038/s41377-023-01278-0

[3] E. Castro-Camus, M. Alfaro M. Photon. Res., **4** (3), 36 (2016). DOI: 10.1364/PRJ.4.000A36

[4] A.E. Yachmenev, D.V. Lavrukhin, I.A. Glinskiy, N.V. Zenchenko, Yu.G. Goncharov, I.E. Spektor, R.A. Khabibullin, T. Otsuji, D.S. Ponomarev. Opt. Eng., **59** (6), 061608 (2019). DOI: 10.1117/1.OE.59.6.061608

[5] A. Singh, A. Pashkin, S. Winnerl, M. Helm, H. Schneider. ACS Photon., **5**, 2718 (2018). DOI: 10.1021/acsphotonics.8b00460

[6] A. Singh, A. Pashkin, S. Winnerl, M. Welsch, C. Beckh, P. Sulzer, A. Leitenstorfer, M. Helm, H. Schneider. Light: Sci. Appl., **9**, 30 (2020). DOI: 10.1038/s41377-020-0265-4

[7] D.H. Auston. Appl. Phys. Lett., **26**, 101 (1975). DOI: 10.1063/1.88079

[8] P.-K. Lu, X. Jiang, Y. Zhao, D. Turan, M. Jarrahi. Appl. Phys. Lett., **120** (26), 261107 (2022). DOI: 10.1063/5.0098340

[9] I.E. Ilyakov, B.V. Shishkin, V.L. Malevich, D.S. Ponomarev, R.R. Galiev, A.Yu. Pavlov, A.E. Yachmenev, S.P. Kovalev, M. Chen, R.A. Akhmedzhanov, R.A. Khabibullin. Opt. Lett., **46** (14), 3360 (2021). DOI: 10.1364/OL.428599

[10] S. Lepeshov, A. Gorodetsky, A. Krasnok, E. Rafailov, P. Belov. Las. Photon. Rev., **11**, 1600199 (2017). DOI: 10.1002/lpor.201600199

[11] C. Berry, N. Wang, M. Hashemi, M. Unlu, M. Jarrahi. Nat. Commun., **4**, 1622 (2013). DOI: 10.1038/ncomms2638

[12] E. Isgandarov, L. Pichon, X. Ropagnol, M.A. El Khakani, T. Ozaki. J. Appl. Phys., **133**, 153102 (2023). DOI: 10.1063/5.0143238

[13] D.S. Ponomarev, D.V. Lavrukhin, I.A. Glinskiy, A.E. Yachmenev, N.V. Zenchenko, R.A. Khabibullin, T. Otsuji, Yu. Goncharov, K.I. Zaytsev. Opt. Lett., **48** (5), 1220 (2023). DOI: 10.1364/OL.486431

[14] A. Gorodetsky, I.T. Leite, E.U. Rafailov. Appl. Phys. Lett., **119** (11), 111102 (2021). DOI: 10.1063/5.0062720

[15] A. Gorodetsky, D.V. Lavrukhin, D.S. Ponomarev, S.V. Smirnov, A. Yadav, R.A. Khabibullin, E.U. Rafailov. IEEE J. Select. Top. Quant. Electron., **29** (5), 8500505 (2023). DOI: 10.1109/JSTQE.2023.3271830

[16] K.A. Kuznetsov, S.A. Tarasenko, P.M. Kovaleva, P.I. Kuznetsov, D.V. Lavrukhin, Yu.G. Goncharov, A.A. Ezhov, D.S. Ponomarev, G.Kh. Kitaeva. Nanomat., **12**, 3779 (2022). DOI: 10.3390/nano12213779

[17] D.V. Lavrukhin, A.E. Yachmenev, I.A. Glinskiy, R.A. Khabibullin, Y.G. Goncharov, M. Ryzhii, T. Otsuji, I.E. Spector, M. Shur, M. Skorobogatiy, K.I. Zaytsev, D.S. Ponomarev. AIP Adv., **9**, 015112 (2019). DOI: 10.1063/1.5081119

[18] D.S. Ponomarev, D.V. Lavrukhin, N.V. Zenchenko, T.V. Frolov, I.A. Glinskiy, R.A. Khabibullin, G.M. Katyba, V.N. Kurlov, T. Otsuji, K.I. Zaytsev. Opt. Lett., **47** (7), 1899 (2022). DOI: 10.1364/OL.452192

[19] I.V. Minin, O.V. Minin, I.A. Glinskiy, R.A. Khabibullin, R. Malureanu, A. Lavrinenko, D.I. Yakubovsky, V.S. Volkov, D.S. Ponomarev. Appl. Phys. Lett., **118**, 131107 (2021). DOI: 10.1063/5.0043923

[20] I.H. Malitson, F.V. Murphy, W.S. Rodney. J. Opt. Soc. Am., **48**, 72 (1958). DOI: 10.1364/JOSA.48.000072

[21] B.Y. Hsieh, M. Jarrahi. J. Appl. Phys., **109**, 084326 (2011). DOI: 10.1063/1.3567909

[22] D.V. Lavrukhin, R.R. Galiev, A.Yu. Pavlov, A.E. Yachmenev, M.V. Maytama, I.A. Glinskiy, R.A. Khabibullin, Yu.G. Goncharov, K.I. Zaytsev, D.S. Ponomarev. Opt. Spectrosc., **126**, 580 (2019). DOI: 10.1134/S0030400X19050199.

[23] D.V. Lavrukhin, A.E. Yachmenev, I.A. Glinskiy, N.V. Zenchenko, R.A. Khabibullin, Yu.G. Goncharov, I.E. Spektor, K.I. Zaytsev, D.S. Ponomarev. Opt. Spectrosc., **128**, 1018 (2020). DOI: 10.1134/S0030400X20070103.

Translated by E.Ilinskaya